

Photoinjection of holes and electrons into sulfur single crystals

Elías López-Cruz,* F. Sánchez-Sinencio,† A. Rose,‡ and J. S. Helman

Departamento de Física, Centro de Investigación del Instituto Politécnico Nacional, Apartado Postal 14-740, México 14, D. F., México

(Received 2 January 1980)

In this work we have made a systematic study of steady-state charge injection into sulfur single crystals by using both uv strongly absorbed light ($\lambda = 350$ nm) and internal-photoemission techniques. The mechanism of charge injection was determined from analysis of the I - V characteristics and their dependence on light intensity. We considered (a) uv hole photoinjection, (b) internal photoemission of holes from an HgS contact, (c) uv electron photoinjection, and (d) internal photoemission of electrons from a Te contact. The results are interpreted using the Mott-Gurney theory. The crystals used had a low density of traps, which allowed us to distinctly observe the transition from the space-charge-limited-current regime to the neutral-contact regime in every case.

I. INTRODUCTION

The study of current injection in solids is a useful tool for the understanding of electronic-transport properties in insulators and it has been used as a standard technique in the characterization of a variety of materials.¹ For sulfur single crystals, the analysis of transient injected currents has been used in the determination of hole and electron mobilities using the following techniques: transient space-charge-limited currents,² transient space-charge-perturbed currents,³ and drift-mobility techniques using light and electron-beam pulses⁴⁻⁷ and x-ray pulses.⁸ Measurements of hole and electron photoinjected currents generated by an internal-photoemission (IP) process have given additional information on the electron transport⁹ and on the valence-band structure¹⁰ of sulfur single crystals. It is accepted that hole drift mobility in sulfur is controlled by traps. Information about traps in this material has been obtained from thermally stimulated conductivity,^{4,7,11,12} by dark injection,¹³ and by steady-state photoinjection.⁵

In this work we have made a systematic study of steady-state charge injection into sulfur single crystals by using both uv strongly absorbed light ($\lambda = 350$ nm) and internal-photoemission techniques. The mechanism of charge injection was determined from analysis of the I - V characteristics and their dependence on light intensity. We considered (a) uv hole photoinjection (UVHP), (b) internal photoemission of holes (IPH) from an HgS contact, (c) uv electron photoinjection (UVEP), and (d) internal photoemission of electrons (IPE) from a Te contact. The results are interpreted using the Mott-Gurney theory. The S_8 crystal used had a low density of traps, which allowed us to distinctly observe the transition from the space-charge-limited-current (SCLC)

regime to the neutral-contact regime in every case.

II. EXPERIMENTAL

Sulfur single crystals were grown by slow evaporation of a saturated solution of sulfur in CS_2 . The evaporation was made at room temperature in the dark during a period of about six weeks. Some of the crystals obtained as explained above were dissolved again in CS_2 and the evaporation process was repeated. Samples produced during the first and second crystallizations are named $T1$ and $T2$, respectively. Platelets about 1 mm thick and 0.5 cm² in area were polished with fine abrasive and lightly etched with benzene. The polished crystals used in all the experiments had a thickness $L = 0.1$ cm and an area $A = 0.5$ cm². For those experiments in which IPH was induced, the crystals were supplied with one black HgS contact prepared as reported in Ref. 10. A Te contact was prepared by vacuum evaporation on those samples used in IPE experiments. The samples were held by a gentle pressure between two conductive quartz plates. All measurements were made at room temperature in an He atmosphere. A 1000-W Xe-Hg lamp with a water filter and a bandpass G-774-3550 Oriel filter was used as a source of uv light or with a water filter and a Balzers interference filter (B-40-495 nm) as a source of visible light. Different light intensities were obtained using various Oriel neutral density filters. Photon fluxes were measured using a thermopile calibrated by NBS. Currents were measured with a 610C Keithley electrometer driving a pen recorder.

Photoinjection of carriers into sulfur was obtained using uv light ($\lambda = 350$ nm) which is strongly absorbed within a few μ m from the illuminated surface of the crystals creating electrons and

holes in that region. The carriers can be pulled selectively from the illuminated surface into the dark region of the crystal using an appropriate bias voltage. We denote by I_h^{uv} and I_e^{uv} the hole and electron uv-induced photocurrents, respectively.

Carriers were also photoinjected by IPH from HgS or IPE from Te into sulfur single crystals illuminating the contact with visible light ($\lambda = 495$ nm) through the sample. When the HgS contact was polarized with a positive voltage the photocurrent I^+ was larger than I^- obtained with a negative bias. The hole photocurrent I_h was obtained by subtracting I^- from I^+ .¹⁰ Conversely, when the Te contact was polarized with a negative voltage the photocurrent I^- was larger than the I^+ obtained with a positive bias. The electron photocurrent I_e was obtained subtracting I^+ from I^- .⁹

All the currents I_h^{uv} , I_e^{uv} , I^+ , and I^- reach a peak value after the onset of light and decrease as a function of time to a steady-state value within 10–120 sec, depending on the applied voltage. The time decay of the currents is associated with the filling of traps in the volume of the sample.

The transit time of electrons was measured using pulsed IPE or pulsed UVEP. A mobility $\mu_e = 6 \times 10^{-4}$ cm²/V sec was obtained in all samples. The transit time of the holes could not be determined because it was shorter than the duration of the available flash ($\tau < 10$ μ sec). Throughout this work we used a hole mobility $\mu_h = 1$ cm²/V sec,¹⁴ and a dielectric constant for sulfur $\epsilon = 3.54 \times 10^{-13}$ F cm⁻¹.

III. THEORY

We assume that the uv light or the internal-photoemission process generates a steady-state carrier concentration N_0 at the surface of the sulfur sample which is independent of the applied voltage V . We are not concerned with the surface-transient processes leading to the final carrier concentration N_0 .

The basic equations which describe the I - V characteristics in the insulator are Poisson's equation

$$\frac{dE}{dx} = \frac{Ne}{\epsilon} \quad (1)$$

and the equation for the current

$$j = (e\mu\theta N + e\mu n)E - eD \frac{dN\theta}{dx}, \quad (2)$$

where $N(x)$ is the density of injected carriers. θ is the ratio between the free and trapped injected charge in thermodynamical equilibrium in the bulk of the insulator. When the trapping is dominated

by a single level in the gap θ is independent of the electric field E . n is the uniform density of thermally generated free carriers in the bulk.

The boundary conditions are

$$\left(\frac{dE}{dx}\right)_s = \frac{N_0 e}{\epsilon} \quad (3)$$

and

$$\int_0^L E(x) dx = V_a - V_p = V, \quad (4)$$

where ϵ is the dielectric constant of the insulator, j is the current density, D is the carrier diffusion constant, L is the thickness of the sample, and V_a the applied voltage. V_p is a polarization voltage due to residual trapped charge Q_t in the bulk of the insulator that cannot be neutralized; thus V is the effective voltage acting on the insulator. The effect of the charge Q_t can also be taken into account by adding Q_t in Poisson's equation instead of introducing V_p in Eq. (4). Both procedures lead to almost the same numerical results; the former, however, is simpler.¹⁵ In our case the diffusion current $eD(dN\theta/dx)$ in Eq. (2) can be disregarded, since it is negligible compared with the conduction current for $V \lesssim 0.025$ V.¹⁶

The system of Eqs. (1)–(4), for $n = 0$, with and without diffusion current was solved exactly in Ref. 16. However, we are interested in keeping n finite, and we find an approximate solution for this case, neglecting the diffusion current. Equations (1) and (2) lead to

$$\frac{dE}{dx} = \frac{j - e\mu n E}{\mu \epsilon \theta E} \quad (5)$$

which can be integrated to give

$$E - E_0 + \frac{j}{e\mu n} \ln\left(\frac{j - e\mu n E}{j - e\mu n E_0}\right) = -\frac{en}{\epsilon \theta} x, \quad (6)$$

where, from Eqs. (3) and (5),

$$E_0 = j/e\mu(n + N_0\theta). \quad (7)$$

Since $E \geq E_0$ and $j \geq e\mu n E$ (the equality holds when the current is due only to the thermally generated carriers), we have

$$0 < (j - e\mu n E)/(j - e\mu n E_0) = 1 - \Delta \leq 1. \quad (8)$$

Using Eq. (7),

$$0 \leq \Delta = e\mu n(E - E_0)/e\mu \theta N_0 E_0 < 1. \quad (9)$$

Keeping terms up to order Δ^2 , Eq. (6) can be written as

$$E = \frac{j}{\mu e(n + N_0\theta)^2} \left[n + \theta N_0 \left(1 + \frac{2\mu e^2(n + N_0\theta)^2 x}{\epsilon \theta j} \right)^{1/2} \right], \quad (10)$$

giving an explicit form for $E(x)$. Equation (4) can be integrated using Eq. (10) to give

$$V = \frac{j}{\mu e(n+N_0\theta)^2} \left\{ nL + \frac{\epsilon \theta^2 N_0 j}{3e^2 \mu (n+N_0\theta)^2} \left[\left(1 + \frac{2\mu e^2 (n+N_0\theta)^2 L}{\epsilon \theta j} \right)^{3/2} - 1 \right] \right\}. \quad (11)$$

It is interesting to analyze the limiting cases of Eq. (11). When $n \ll N_0\theta$, then for $A = 2\mu e^2 \theta N_0^2 L / \epsilon j \gg 1$ we obtain

$$j = 9\mu \epsilon \theta V^2 / 8L^3 \quad (12)$$

which describes a space-charge-limited current¹⁷ independent of N_0 and proportional to V^2 . For $A \ll 1$, we obtain

$$j = \epsilon \mu \theta N_0 V / L \quad (13)$$

which is linear in V and corresponds to a neutral contact.¹⁸

On the other hand, for $N_0\theta \ll n$ we obtain

$$j = (e\mu n V / L)(1 + \theta N_0 / n)^2 \quad (14)$$

which corresponds to an Ohmic current.

For fitting purposes, it is convenient to shorten Eq. (11) and to write

$$v = KZ + Z^2[(1 + 1/Z)^{3/2} - 1], \quad (15)$$

where

$$v = (3\epsilon / 4eN_0L^2)V, \quad (16)$$

$$Z = \epsilon \theta j / 2\mu e^2 L (n + \theta N_0)^2, \quad (17)$$

and

$$K = 3n / 2\theta N_0. \quad (18)$$

Equation (15) has been used to describe the mechanism of photoinduced discharge in sulfur single crystals,¹⁹ where the conditions $K \approx 1$ prevail. The conditions of the present experiment correspond to $K \ll 1$. Thus we set $K = 0$ and

$$Z = \epsilon j / 2\mu e^2 \theta N_0^2 L, \quad (19)$$

and Eq. (15) reduces to Eq. (27) of Ref. 16.

We now describe the case of deep trapping in the absence of thermally generated carriers. Equations (1), (3), and (4) remain the same and Eq. (2) now takes the form

$$j = e\mu\nu E, \quad (20)$$

where ν is the density of free carriers, which in the case of deep trapping is related to N by an expression of the form¹⁸

$$\nu = B_1 N^m. \quad (21)$$

Here B_1 and m are adjustable parameters.

Equations (1) and (20) can be integrated with the boundary conditions (3) and (4) to give

$$V - V_p = \frac{4m}{2m+1} L^2 \left(N_0 \frac{e}{\epsilon} \right)^{3-2m} x^2 \left[\left(\frac{m+1}{2m} \frac{(N_0 e / \epsilon)^{m+1}}{x} + 1 \right)^{(2m+1)/(m+1)} - 1 \right] \quad (22)$$

with

$$x = j / 2\mu e B_1 N_0^2 L (e/\epsilon)^{2-m}. \quad (23)$$

For $m = 1$ and $n = 0$, Eq. (22) coincides with Eq. (15). For $[(m+1)/2mx](N_0 e/\epsilon)^{m-1} \gg 1$ we obtain the limit of SCLC,

$$j = 2eL\mu B_1 \left(\frac{\epsilon}{e} \right)^m \left[\frac{2m+1}{4m} \left(\frac{2m}{m+1} \right)^{(2m+1)/(m+1)} / L^2 \right]^{m+1} V^{m+1}, \quad (24)$$

and for $[(m+1)/2mx](N_0 e/\epsilon)^{m-1} \ll 1$ we obtain the limit of a neutral contact

$$j = e\mu B_1 N_0^m V / L. \quad (25)$$

IV. RESULTS AND DISCUSSION

A. UVHP

The I - V characteristic of I_h^{uv} in sample T1 at four light intensities $0.1F_0$, $0.3F_0$, F_0 , and $3.5F_0$ are shown in Fig. 1. Here, $F_0 = 2.2 \times 10^{17}$ photons $\text{cm}^{-2} \text{sec}^{-1}$. The dependence of I_h^{uv} on the light in-

tensity at 100 V is shown in Fig. 2.

The full lines in Fig. 1 correspond to the fitting of I_h^{uv} - V using Eq. (15). The fitting yields the values $n = 0$, $\theta = 1.05 \times 10^{-5}$, $N_0 = 4.9 \times 10^{10} F / F_0 \text{ cm}^{-3}$, and $V_p = 50$ V. Notice that N_0 is proportional to F within the range of light intensities used.

The above parameters were used to calculate the theoretical I vs F curve shown in Fig. 2 (full line). μ_h may vary up to a factor of order 5 from sample to sample⁷; however, the formulas depend only on the product $\theta\mu_h$, so that the fitting would not be affected; only the value of θ would be

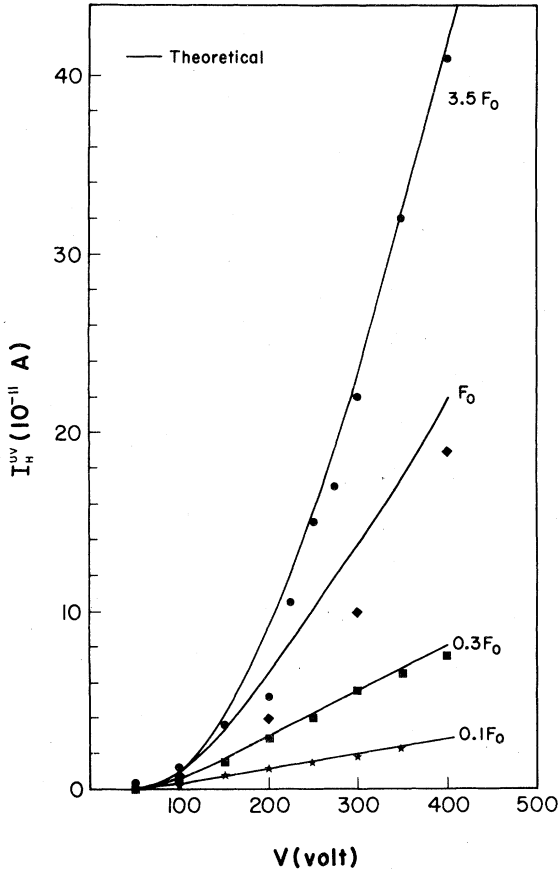


FIG. 1. uv hole photocurrent I_h^{uv} versus applied voltage for four different light intensities. $F_0 = 2.2 \times 10^{17}$ photons $\text{cm}^{-2}\text{sec}^{-1}$. The full lines correspond to the theoretical model proposed in Sec. IV.

changed by the reciprocal of that factor.

At low light intensities ($0.1F_0$) the linear I - V characteristic corresponds to a neutral contact; the SCLC region cannot be observed within our experimental resolution. The transition from an SCLC characteristic to a neutral-contact char-

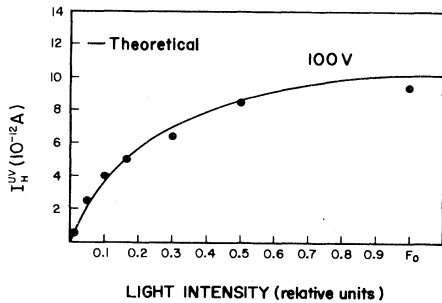


FIG. 2. I_h^{uv} as a function of light intensity. The applied voltage is $V_a = 100$ V. The full line corresponds to the theoretical model proposed in Sec. IV.

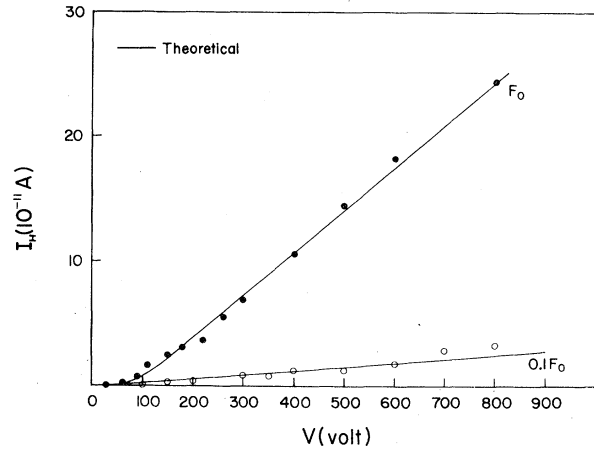


FIG. 3. Current due to internal photoemission of holes (I_h) from HgS into S_α versus applied voltage for two different light intensities. $F_0 = 2.4 \times 10^{16}$ photons $\text{cm}^{-2}\text{sec}^{-1}$. The full lines correspond to the theoretical model proposed in Sec. IV.

acteristic is apparent at high light intensities ($3.5F_0$). No Ohmic region at low voltages is observed ($n=0$). V_p was identified with the applied voltage for which the current changes sign.

B. IPH

Measurements of I_h by IPH were made on the

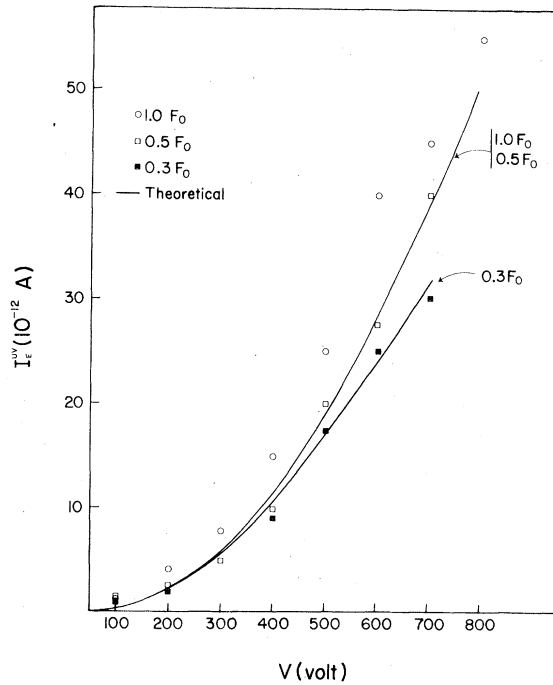


FIG. 4. uv electron photocurrent I_e^{uv} vs V for three light intensities $0.3F_0$, $0.5F_0$, and F_0 . Here $F_0 = 7.7 \times 10^{17}$ photons $\text{cm}^{-2}\text{sec}^{-1}$. The full lines were calculated using the model proposed in Sec. IV.

same sample used in the UVHP experiments. The characteristic I_h - V using steady-state values of I_h at the two light intensities F_0 and $0.1F_0$, where $F_0 = 2.4 \times 10^{16}$ photons $\text{cm}^{-2} \text{sec}^{-1}$, is shown in Fig. 3. The full lines correspond to the fitting of I_h vs V using Eq. (15); the fitting yields the values $n=0$, $\theta = 1.05 \times 10^{-5}$, $N_0 = 2.0 \times 10^{10} F/F_0 \text{ cm}^{-3}$, and $V_p = 50 \text{ V}$.

At low light intensities ($0.1F_0$) the linear I - V characteristic corresponds to a neutral contact; the SCLC region cannot be observed within the voltage range. The transition from an SCLC characteristic to a neutral-contact characteristic is apparent at high light intensities (F_0). Measurements of I_h vs F at constant voltage were also in agreement with Eq. (15) with the above parameters.

C. UVEP

The characteristic I_e^{uv} - V in sample T1 at three light intensities $0.3F_0$, $0.5F_0$, and F_0 , where $F_0 = 7.7 \times 10^{17}$ photons $\text{cm}^{-2} \text{sec}^{-1}$, are shown in Fig. 4. The full lines correspond to the fitting of I_e^{uv} vs V using Eq. (15). The fitting yields the values $n=0$, $\theta = 4 \times 10^{-4}$, $N_0 = 9.6 \times 10^{11} F/F_0 \text{ cm}^{-3}$, and $V_p = 50 \text{ V}$.

Within the range of electric fields used here ($E < 8000 \text{ V/cm}$) and for $F \geq 0.5F_0$, the I - V characteristics are independent of F corresponding to

SCLC. For $F = 0.3F_0$ the transition from SCLC to neutral contact is apparent.

D. IPE

I_e was measured in sample T2 and the characteristics I_e - V at five light intensities $0.05F_0$, $0.1F_0$, $0.3F_0$, $0.5F_0$, and $F_0 = 2.4 \times 10^{16}$ photons $\text{cm}^{-2} \text{sec}^{-1}$ are shown in Fig. 5. The graph also shows a characteristic I_e^{uv} - V corresponding to the same sample for a uv light intensity of 7.7×10^{17} photons $\text{cm}^{-2} \text{sec}^{-1}$. Figure 6 shows I_e as a function of F at 300 V. For sample T2 the SCLC characteristic behaves like $I_e \propto V^{4.1}$, which indicates the presence of an exponential distribution of traps in the bulk.

It is not possible to obtain an overall fitting of the data for I_e vs V using Eq. (22) with N_0 independent of V . Discrepancies up to a factor of 2 are seen for low light intensities ($F \leq 0.1F_0$) above 300 V. In view of this we used the experimental data together with Eq. (22) to determine N_0 as a function of voltage and light intensity. The fitting now yields $n=0$, $m=3.1$, $B_1 = 2.45 \times 10^{-25} (\text{cm}^3)^{m-1}$, and $V_p = 50 \text{ V}$. N_0 as a function of V and F is plotted in Fig. 7. The full lines in Fig. 5 represent the theoretical I - V curves. At low voltages N_0 is independent of V and proportional to F as in the previous cases. However, for high voltages N_0

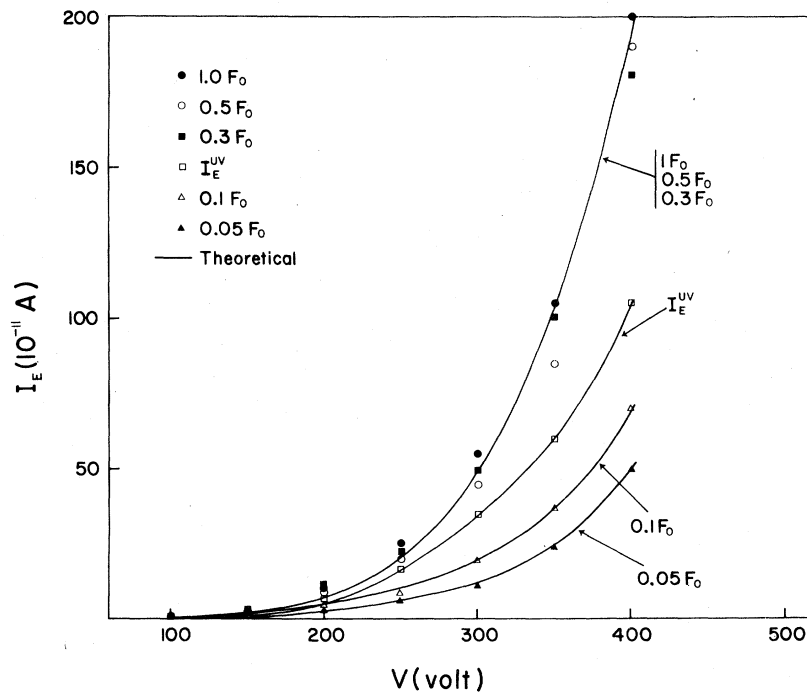


FIG. 5. Current due to internal photoemission of electrons (I_e) from Te into S_α versus applied voltage for five light intensities $F_0 = 2.4 \times 10^{16}$ photons $\text{cm}^{-2} \text{sec}^{-1}$. Here are also shown results of injection of electrons using uv light " I_e^{uv} ," in this case $F = 7.7 \times 10^{17}$ photons $\text{cm}^{-2} \text{sec}^{-1}$. The full lines were calculated with the theoretical model of Sec. IV.

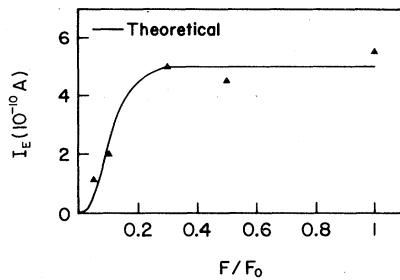


FIG. 6. I_e as a function of light intensity. $F_0 = 2.4 \times 10^{16}$ photons $\text{cm}^{-2} \text{sec}^{-1}$. The applied voltage is $V_a = 300$ V. The full line was calculated using Eq. (22).

increases as if a voltage-dependent injection process begins to dominate the internal photoemission from the Te. This effect is negligible at high levels of illumination. We speculate that this effect is related to charge photoinjection from surface traps.²⁰

V. CONCLUSIONS

We have shown that both photocurrents and internal-photoemission currents in sulfur single crystals with a low concentration of traps can be understood in terms of the Mott-Gurney¹⁶ theory. The fitting of the experimental values yields the density of carriers at the injecting contacts, the bulk density of deep traps, and the ratio between free and trapped charge in thermodynamical equilibrium.

Since photocurrents and internal-photoemission currents are responsible for the photodischarge of insulators, the results presented here allow a

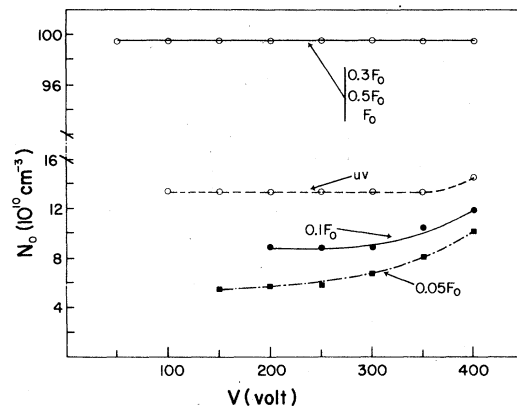


FIG. 7. N_0 as a function of the applied voltage. These data were obtained by fitting the experimental points of Fig. 5 using Eq. (22). Note the change of scale above $16 \times 10^{10} \text{ cm}^{-3}$.

detailed description of the photodischarge of sulfur single crystals with low density of traps.¹⁹

ACKNOWLEDGMENTS

We acknowledge many helpful discussions with Professor A. Many, Professor G. F. L. Ferreira, Professor B. S. H. Royce and Professor C. Menezes. We thank P. García and J. García-Coronel for their technical assistance. This work was partially supported by CONACyT (Conseja Nacional de Ciencia y Tecnología), PNCB (Programa Nacional de Ciencias Básicas)-CONACyT, and SEPAFIN [Secretaría de Patrimonio y Fomento Industrial (Comisión Nacional de Energéticos)], México.

*Present address Instituto de Ciencias, Universidad Autónoma de Puebla, Apartado J-48, Puebla, Pue., México.

†Also at Escuela Superior de Física y Matemáticas, I.P.N., México.

‡Permanent address: Boston University, U. S. A.

¹Murray A. Lampert and Peter Mark, *Current Injection in Solids* (Academic, New York, 1970).

²A. Many, M. Simhony, and Y. Grushkevitz, *J. Phys. Chem. Solids* **26**, 1925 (1965).

³D. J. Gibbons and A. C. Papadakis, *J. Phys. Chem. Solids* **29**, 115 (1968).

⁴A. R. Adams and W. E. Spear, *J. Phys. Chem. Solids* **25**, 1113 (1964).

⁵K. K. Thornber and C. A. Mead, *J. Phys. Chem. Solids* **26**, 1489 (1965).

⁶D. J. Gibbons and W. E. Spear, *J. Phys. Chem. Solids* **27**, 1917 (1966).

⁷W. D. Gill, G. B. Street, and R. E. McDonald, *J. Phys. Chem. Solids* **28**, 1517 (1967).

⁸Yasutaka Watanabe, Nobuyuki Saito, and Yoshio Inuishi, *J. Phys. Soc. Jpn.* **25**, 1081 (1968).

⁹R. Williams and F. Sánchez-Sinencio, *J. Chem. Phys.*

52, 3216 (1970).

¹⁰J. González-Basurto, F. Sánchez-Sinencio, and J. S. Helman, *Phys. Rev. B* **6**, 3865 (1972).

¹¹F. Sánchez-Sinencio, S. Mascarenhas, and B. S. H. Royce, *Phys. Lett.* **26A**, 70 (1967).

¹²A. Ferreira-Gómez and F. Sánchez-Sinencio, *Phys. Lett.* **34A**, 130 (1971).

¹³F. Lohmann and W. Mehl, *J. Phys. Chem. Solids* **28**, 1317 (1967).

¹⁴W. E. Spear and A. R. Adams, in *Elemental Sulfur*, edited by B. Meyer (Interscience, New York, 1965).

¹⁵Guilherme Fontes Leal Ferreira, private communication.

¹⁶N. F. Mott and R. W. Gurney, *Electronic Processes in Ionic Crystals* (Dover, New York, 1964).

¹⁷A. Rose, *Phys. Rev.* **97**, 1538 (1955).

¹⁸A. Rose, *Concepts in Photoconductivity and Allied Problems* (Interscience, New York, 1963).

¹⁹F. Sánchez-Sinencio, E. López-Cruz, and J. S. Helman, *Bull. Am. Phys. Soc.* **24**, 244 (1979). An extended version is planned to be published elsewhere.

²⁰Yuzo Mizobuchi, Hiromu Kato, and Ryuichi Shintani, *J. Phys. Soc. Jpn.*, **30**, 1374 (1971).